Monte Carlo simulation of ferroelectricity induced by collinear magnetic order in Ising spin chain

Xiaoyan Yao[1,2] and Veng Cheong Lo[1,a)]
[1]*Department of Applied Physics, The Hong Kong Polytechnic University, Hong Kong, China*
[2]*Department of Physics, Southeast University, Nanjing 211189, China*

(Received 22 July 2008; accepted 12 September 2008; published online 31 October 2008)

To understand the collinear-magnetism-driven ferroelectricity in the frustrated Ising spin chain, the fascinating magnetoelectric behavior is investigated by using Monte Carlo simulation based on one dimensional elastic Ising model. Our simulation quantitatively reproduces the experimental results of the complicated electric and magnetic behaviors as functions of temperature observed in Ca_3CoMnO_6 compound [Phys. Rev. Lett. **100**, 047601 (2008)]. Moreover, the short-ranged up-up-down-down magnetic ordering is confirmed to be the origin of electric polarization, and the curves of energy components dependent on temperature provide a reasonable explanation for the unconventional magnetoelectric phase transition revealed in the Ising chain magnet. © *2008 American Institute of Physics*. [DOI: 10.1063/1.3009321]

I. INTRODUCTION

Due to the potential applications and fundamental academic curiosity, the investigation of multiferroic materials, especially magnetoelectric (ME) coupling compounds, has attracted considerable attention in recent years. In particular, the magnetism-driven ferroelectricity was discovered in many frustrated systems, which renewed the interest of investigation in this field.[1–5] As revealed in these compounds, the strong coupling between the electric polarization and the magnetic ordering provides a possibility of simultaneously controlling magnetic and electric degrees of freedom. In order to achieve their potential applications, it is very essential to understand how these two degrees of freedom are coupled to each another at a microscopic level. Unfortunately the corresponding microscopic mechanism has not been unveiled until now.

The noncollinear magnetic phase, especially the spiral spin ordering, is a common way to magnetism-driven ferroelectricity. Microscopically, the ME mechanism of the spin current[6] and the Dzyaloshinskii–Moriya interaction[7,8] were proposed for these noncollinear magnets. Besides the noncollinear magnetism, other magnetic orderings are also possible routes toward ME coupling and ferroelectricity generation.[9] However their true origin is still equivocal and remains an interesting topic. A recent experiment of Choi *et al.*[10] reported the discovery of ferroelectricity in the Ising chain magnet $Ca_3Co_{2-x}Mn_xO_6$ ($x \approx 0.96$ very near 1), convincingly confirming that the collinear spin order can generate ferroelectricity. It was supposed that the movements of magnetic ions resulting from exchange striction based on an up-up-down-down spin ordering induce the electric polarization.[10,11] This theoretical prediction needs further evidence, and more detailed investigations on the interplay between the ferroelectric and magnetic ordering would be very helpful to illustrate this novel behavior. In this paper, we construct a one dimensional (1D) elastic Ising model to investigate the ME properties of Ca_3CoMnO_6 by Monte Carlo (MC) simulation. The simulation results qualitatively reproduce the main characteristics of electric and magnetic behaviors in Ca_3CoMnO_6, confirming that the ferroelectricity in this compound is driven by collinear magnetism. We believe that the present work would help understand the ferroelectricity in a frustrated magnet, and shed light for potential applications. In fact, as far as we know, few works on the MC simulation of such collinear-magnetism-driven ferroelectricity have been reported.

II. THEORY AND MODELING

Ca_3CoMnO_6, belonging to the family of 1D spin-chain materials, can be regarded as a doped compound of $Ca_3Co_2O_6$, which represents one of the most frequently studied compounds due to its complex magnetic properties.[12,13] With half of Co ions replaced by Mn ions, Ca_3CoMnO_6 consists of parallel 1D $CoMnO_6$ chains, aligned along the hexagonal *c*-axis and separated by Ca^{2+} ions. It forms a triangular lattice in the *ab*-plane. Each spin chain is composed of alternatively face-sharing CoO_6 trigonal prisms and MnO_6 octahedra along the *c* axis where the Co^{2+} ion is the low-spin and Mn^{4+} ion is the high-spin.[10,14] Due to the much stronger intrachain interaction than the interchain one and the strong Ising-like anisotropy, this compound can be characterized by a 1D Ising model.[10,14] Based on the former investigation,[11,15] the ferromagnetic (FM) coupling ($J_{FM} > 0$) between each nearest-neighboring Mn–Co spin pair and the next-nearest-neighbor antiferromagnetic (AFM) interaction are considered in order to generate spin frustration and accordingly produce the up-up-down-down spin structure. Since the magnetic moment of Mn ion is about three times larger than that of Co, that is 1.93 μ_B and 0.66 μ_B for Mn and Co ions, respectively.[10] The AFM coupling between each next-nearest-neighboring Mn–Mn pair should be stronger than that for Co–Co ($J_{AF_{Mn}} < J_{AF_{Co}} < 0$). For simplicity, $J_{AF_{Mn}} = 9\ J_{AF_{Co}}$ is assumed. In addition, in the pure up-up-down-

a)Author to whom correspondence should be addressed. Electronic mail: timothy.lo@polyu.edu.hk.

TABLE I. System parameters chosen for the simulation.

Parameter	Value	Parameter	Value
J_{FM_0}	90	η	−8
$J_{\mathrm{AF}_{\mathrm{Mn}}}$	−65.7	k	34 000
$J_{\mathrm{AF}_{\mathrm{Co}}}$	−7.3	g	2

down spin state the exchange striction has no effect on the next-nearest-neighboring spins, therefore the exchange striction is only considered for J_{FM} here. No matter what form of distance dependence for J_{FM} between the nearest-neighboring spins is, it can be expanded to the following linear approximation form:

$$J_{\mathrm{FM}}(r_{i,i+1}) = J_{\mathrm{FM}_0}\left(1 + \eta\frac{r_{i,i+1} - r_0}{r_0}\right) = J_{\mathrm{FM}_0}[1 + \eta(d_{i+1} - d_i)], \quad (1)$$

where J_{FM_0} is defined as the bare FM spin-spin interaction, and η gives the strength of the coupling between the spins and the displacements. $\eta<0$ reflects that the interaction gets stronger as the spins get closer to each other, and vice versa. r_0 is the original distance between two ions without the exchange striction, $r_{i,i+1}$ is the distance between the ith ion, and the $(i+1)$th is the ion under the exchange striction. d_i denotes the displacement of the ith ion normalized by r_0 and it bears a positive value when this ith ion is approaching the $(i+1)$th one. According to Eq. (1), the change in J_{FM} is related to the change in the distance between the spins, therefore the relative movement of the ions is the key for the exchange striction. For simplicity, it is assumed that only Co ions move, namely, $d_i \neq 0$ for Co, but $d_i=0$ for Mn case. The Hamiltonian of this 1D Ising model can be written as

$$H = -\sum_{\langle i,j\rangle} J_{\mathrm{FM}}(r_{ij}) S_i S_j - \sum_{[i,k]}^{\mathrm{Mn}} J_{\mathrm{AF}_{\mathrm{Mn}}} S_i S_k - \sum_{[i,k]}^{\mathrm{Co}} J_{\mathrm{AF}_{\mathrm{Co}}} S_i S_k - hg\mu_B \sum_i S_i - E\sum_i q d_i + \frac{1}{2}k\sum_i d_i^2 \quad (2)$$

where $S_i = \pm 1$ represents the ith spin of the chain, $\langle i,j\rangle$ denotes the summation over all the nearest-neighboring spin pairs, and $[i,j]$ signifies that over all the next-nearest-neighboring pairs, which is calculated for Mn and Co respectively. h is the external magnetic field applied along the direction of spin chain, g is the Lande factor, and μ_B is the Bohr magnetron. E is the electric field also applied along the chain and q is the charge state of the moving ions, that is $q=2$ for Co^{2+}. The last term on the right of Eq. (2) is the elastic energy presented in the form of the harmonic potential, where k is the elastic constant with the value large enough to ensure the small values of the ionic displacements. For convenience, k_B is chosen to be unity, and the other parameters are scaled by the above assumption. The values of these parameters for the simulation are shown in Table I. Since the real values of these parameters are not available from experiments, they are chosen by the qualitative comparison between the simulated results and the experimental data.

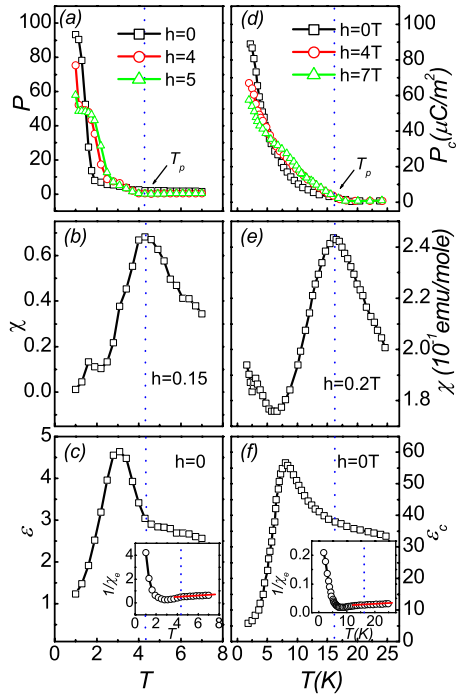

FIG. 1. (Color online) (a) Polarization P against temperature T for different h values along the chain. (b) Temperature dependence of χ under a small magnetic field $h=0.15$ along the chain direction. (c) Dielectric constant ε against T. The insert gives $1/\chi_e$ as a function of T, and the red line presents its linear behavior in the high T-range. The corresponding experimental results of P_c, χ, and ε_c in $Ca_3Co_{2-x}Mn_xO_6$ ($x\approx 0.96$) are plotted in (d)–(f), respectively. (The insert in (f) shows $1/\chi_e$ as a function of T). Reproduced from Ref. 10.

The MC simulation is performed on a 1D Ising spin chain (of the system size $L=4000$) with periodic boundary condition. The spin and the displacement are updated according to the Metropolis algorithm, respectively. Similar to the measurement process in the experiment,[10] the system is initially polarized by a large electric field of $E=160$ at low temperature ($T=1$). Then as T is raised, electric polarization (P) and dc magnetic susceptibility ($\chi=M/h$) along the chain are calculated under different h in the presence of a small applied electric field ($E=1$). For every T, the initial 300 000 MC steps (MCS) are discarded for equilibration, and then the results are obtained by averaging 10 000 data. Each date is collected at every 5 MCS. During this process the electric susceptibility χ_e along the chain is calculated based on the statistic fluctuation, namely,[16]

$$\chi_e = \frac{\langle P^2\rangle - \langle P\rangle^2}{T}. \quad (3)$$

Then the relative dielectric constant (ε) is calculated by

$$\varepsilon = \chi_e + 1. \quad (4)$$

The final results are obtained by averaging more than ten independent data sets obtained by selecting different seeds for random number generation.

III. RESULTS AND DISCUSSION

Our simulation results are presented on the left column of Fig. 1, and the corresponding experimental data from Choi

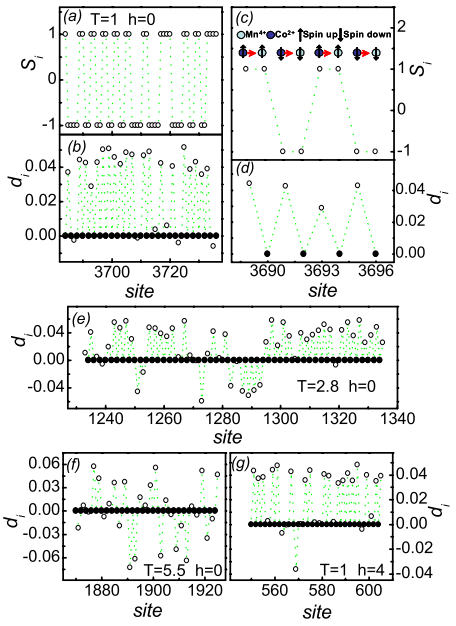

FIG. 2. (Color online) (a) Partial snapshot of spins in a chain for $h=0$ and $T=1$, and (b) the corresponding snapshot for the displacement of ions, (c) enlarged view of spins extracted from the snapshot in (a) over eight ionic sites, and (d) enlarged view of the corresponding displacement extracted from the snapshot in (b). The sketches of these eight ions are presented on the top of (c). Partial displacement snapshots of the chain are plotted in (e) at $h=0$ and $T=2.8$, (f) at $h=0$ and $T=5.5$, and (g) at $h=4$ and $T=1$.

et al.[10] are shown on the right column in order to draw a convenient comparison. It can be seen that our simulation result is qualitatively in good agreement with experimental data, which is presented in the following three aspects. First, Fig. 1(a) demonstrates the simulated $P(T)$ curves under different h. Even when $h=0$, P gradually emerges below the transition temperature $T_p \approx 4.3$, then rises rapidly below a lower T. The application of h along the chain has a complicated influence on the ferroelectric behavior of the system, namely, h suppresses P when T is below 1.5, but it enhances P above that temperature. Second, as shown in Fig. 1(b), a broad peak in $\chi(T)$ curve appears at T_p under a weak magnetic field $h=0.15$ along the chain direction, indicating the transition from AFM to paramagnetic phase, and a very small peak occurs at a lower T. Third, in Fig. 1(c) the curve of ε against temperature deviates from its high-temperature behavior at T_p, and then reveals a broad peak at a lower T followed by a sharp drop on decreasing T, which is discussed in more detail in the following paragraph. In the insert of Fig. 1(c), the reciprocal of χ_e follows the Curie–Weiss law above T_p, demonstrating the linear paraelectric behavior. Comparing with the experimental results on the right column [Figs. 1(d)–1(f)], it is clear that the main electric and magnetic characteristics of Ca_3CoMnO_6 obtained from the experiments can be qualitatively reproduced by this 1D elastic Ising model.

As suggested by Choi *et al.*,[10] the emergence of P attributes to the exchange striction in an up-up-down-down magnetic structure. This argument is supported by our simulation and a more extensive scenario is displayed here. Figures 2(a) and 2(b) demonstrate the snapshots for the partial spin and displacement at $T=1$ and $h=0$, extracted from our simulation. Figures 2(c) and 2(d) display the enlarged views over eight ion sites in Figs. 2(a) and 2(b), and the corresponding sketches of these eight ions are presented on the top of Fig. 2(c). As shown in Fig. 2(c), a typical up-up-down-down spin state emerges due to the spin frustration. The spin frustration originates from the competition between the nearest-neighbor FM and next-nearest-neighbor AFM interactions. Consequently, the exchange striction, which shrinks the bond lengths between the parallel spins and stretches those between the antiparallel spins, results in the movements of ions along the chain. As shown in Fig. 2(d), the hollow circles denote the mobile Co ions moving along the chain, and the solid ones represent the immobile Mn ions. While the two opposite displacement directions are equally probable in this system without electric field,[10] a high polarizing electric field imposes a dominant direction for these displacements. Therefore many ferroelectric domains clamped with the magnetic domains of up-up-down-down ordering are formed, and then a macroscopic P emerges. As illustrated in Fig. 2(a), the short-ranged feature of up-up-down-down ordering is also consistent with the neutron diffraction experiment.[10] At low T, these polarized domains are frozen due to the spin frustration. However with T increasing toward T_p, the frozen domains gradually melt and the displacements of ions cannot keep to the polarized direction anymore, as shown in Fig. 2(e). The counteraction between the polarized domains with two opposite directions leads to the sharp decrease in macroscopic polarization. Besides, these melting domains are sensitive to the electric field, namely, a small electric field may make these domains aligned along the same direction and consequently P increases, which results in the peak of ε. As T is raised to T_p, the short-ranged up-up-down-down AFM state collapses, where χ shows a broad peak, and then P fades away gradually. When T above T_p, the ionic displacements show a disorder paraelectric character as presented in Fig. 2(f), which coincides with the linear behavior of the reciprocal of χ_e [Fig. 1(c)].

The temperature dependence of the electric and magnetic properties can be further understood by analyzing the energy of the system. In order to study this dependence, the main components of energy are listed in the following:

$$H_{\mathrm{FM}} = -\sum_{\langle i,j \rangle} J_{\mathrm{FM}}(r_{ij}) S_i S_j, \tag{5}$$

$$H_{\mathrm{AF}} = -\sum_{[i,k]}^{\mathrm{Mn}} J_{\mathrm{AF_{Mn}}} S_i S_k - \sum_{[i,k]}^{\mathrm{Co}} J_{\mathrm{AF_{Co}}} S_i S_k, \tag{6}$$

$$H_{\mathrm{M}} = -hg\mu_B \sum_i S_i, \tag{7}$$

$$H_{\mathrm{el}} = \tfrac{1}{2} k \sum_i d_i^2. \tag{8}$$

Equations (5)–(8) respectively represent the FM energy between the nearest-neighbor spins, the AFM energy between the next-nearest-neighbor pairs, the magnetic energy, and the elastic energy induced by ionic movements. The temperature

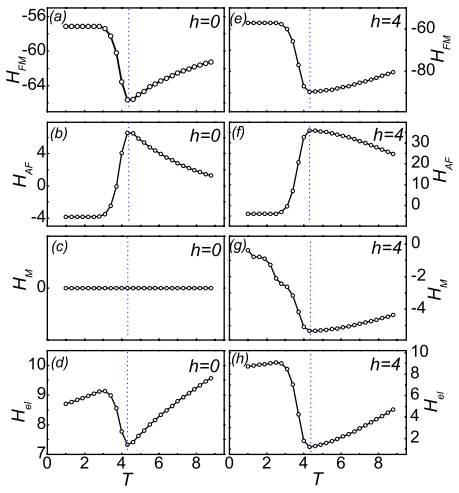

FIG. 3. (Color online) (a) H_{FM}, (b) H_{AF}, (c) H_M and (d) H_{el} as functions of T when $h=0$ in the left column. Correspondingly, (e) H_{FM}, (f) H_{AF}, (g) H_M, and (h) H_{el} as functions of T under $h=4$ are plotted in the right column.

dependence of these energies at $h=0$ and $h=4$ are respectively shown on the left and right columns in Fig. 3. The competition of different energies induces the phase transition taking place at T_p. In Figs. 3(a), 3(b), and 3(d), H_{FM}, H_{AFM}, and H_{el} all exhibit anomalies at T_p. In particular, H_{FM} and H_{el} are minima, while H_{AF} attains maxima. It is implied that the up-up-down-down AFM state collapses and the exchange striction is the weakest at this temperature. Consequently the movements of ions are suppressed. In a macroscopic view, P disappears, and χ presents a broad peak denoting the AFM transition. When the magnetic field of $h=4$ is applied along the chain, H_{FM} is lower but H_{AF} is higher than those with $h=0$ as shown in Figs. 3(e) and 3(f). It is indicated that h suppresses the up-up-down-down state and also the exchange striction [Fig. 3(h)]. Accordingly, the displacements of ions are also suppressed to a certain extent as demonstrated in Fig. 2(g). It is worthwhile to note that h results in the stepwise nature of H_M [Fig. 3(g)], which creates several inflexions of $P(T)$ graphs under magnetic field. Moreover, $P(T)$ curves of different h cross each other.

IV. CONCLUSION

In summary, the collinear-magnetism-driven ferroelectricity in a frustrated Ising spin chain with the competing nearest-neighbor FM and next-nearest-neighbor AFM couplings is investigated by using MC simulation. The simulation result is qualitatively consistent with the experimental results. The electric and magnetic properties obtained in our simulation present a clear scenario of the complicated ME behaviors observed in Ca_3CoMnO_6. The snapshots of ionic spins and displacements confirm that the ferroelectricity in this compound is induced by a collinear magnetic ordering. Also the temperature dependence of different energy components is discussed to further understand the exotic ME transition. Although the real material is far more complicated than the present model, the simulated results are believed to cast some light on the understanding of the ferroelectricity driven by the collinear magnetic ordering in the frustrated system.

ACKNOWLEDGMENTS

We thank Qingchang Li, Shuai Dong and Yunjun Guo for helpful discussion. This work is supported by the research grants from the Hong Kong Polytechnic University (Grant No. 1-ZV44) and the National Natural Science Foundation of China (Grant No. 10747115).

[1] K. Taniguchi, N. Abe, T. Takenobu, Y. Iwasa, and T. Arima, Phys. Rev. Lett. **97**, 097203 (2006).
[2] S. Park, Y. J. Choi, C. L. Zhang, and S.-W. Cheong, Phys. Rev. Lett. **98**, 057601 (2007).
[3] G. Lawes, A. B. Harris, T. Kimura, N. Rogado, R. J. Cava, A. Aharony, O. Entin-Wohlman, T. Yildrim, M. Kenzelmann, C. Broholm, and A. P. Ramirez, Phys. Rev. Lett. **95**, 087205 (2005).
[4] T. Kimura, G. Lawes, and A. P. Ramirez, Phys. Rev. Lett. **94**, 137201 (2005).
[5] T. Kimura, T. Goto, H. Shintani, K. Ishizaka, T. Arima, and Y. Tokura, Nature (London) **426**, 55 (2003).
[6] H. Katsura, N. Nagaosa, and A. V. Balatsky, Phys. Rev. Lett. **95**, 057205 (2005).
[7] I. A. Sergienko and E. Dagotto, Phys. Rev. B **73**, 094434 (2006).
[8] Q. C. Li, S. Dong, and J.-M. Liu, Phys. Rev. B **77**, 054442 (2008).
[9] I. A. Sergienko, C. Sen, and E. Dagotto, Phys. Rev. Lett. **97**, 227204 (2006).
[10] Y. J. Choi, H. T. Yi, S. Lee, Q. Huang, V. Kiryukhin, and S.-W. Cheong, Phys. Rev. Lett. **100**, 047601 (2008).
[11] S.-W. Cheong and M. Mostovoy, Nature Mater. **6**, 13 (2007).
[12] X. Y. Yao, S. Dong, and J.-M. Liu, Phys. Rev. B **73**, 212415 (2006); X. Y. Yao, S. Dong, H. Yu, and J.-M. Liu, *ibid.* **74**, 134421 (2006); X. Y. Yao, S. Dong, K. Xia, P. L. Li, and J.-M. Liu, *ibid.* **76**, 024435 (2007).
[13] V. Hardy, M. R. Lees, O. A. Petrenko, D. McK. Paul, D. Flahaut, S. Hébert, and A. Maignan, Phys. Rev. B **70**, 064424 (2004).
[14] V. G. Zubkov, G. V. Bazuev, A. P. Tyutyunnik, and I. F. Berger, J. Solid State Chem. **160**, 293 (2001).
[15] M. E. Fisher and W. Selke, Phys. Rev. Lett. **44**, 1502 (1980).
[16] V. Privman, *Finite Size Scaling and Numerical Simulation of Statistical System* (World Scientific, Singapore, 1990).